Water Practice & Technology

IWA PUBLISHING

Water Practice & Technology Vol 18 No 10, 2277 doi: 10.2166/wpt.2023.147

Process optimization of anionic dye (Melioderm HF Brown G) removal from aqueous solution utilizing adsorbent prepared from *Labeo rohita* fishbone

Md. Arafat Hossain[a], Plabon Islam Turzo[b], Md. Saidur Rahman Shakil[b] and Fatema Tuj-Zohra [a,*]

[a] Department of Leather Products Engineering, Institute of Leather Engineering and Technology, University of Dhaka, 44-50, Hazaribagh, Dhaka 1209, Bangladesh
[b] Department of Leather Engineering, Institute of Leather Engineering and Technology, University of Dhaka, 44-50, Hazaribagh, Dhaka 1209, Bangladesh
*Corresponding author. E-mail: fatema.ilet@du.ac.bd

FT-Z, 0000-0002-2298-9978

ABSTRACT

In this study, the prepared bio-adsorbents from *Labeo rohita* fishbones were used to remove the anionic acid dye Melioderm HF (High Fastness) Brown G (MHFB) from the aqueous solution. Scanning electron microscopy (SEM) and Fourier-transform infrared spectroscopy (FTIR) were used to analyze the morphology and chemical composition of fishbone powder (FBP) before and after MHFB dye adsorption. In a batch experiment, factors such as initial dye concentration (100–250 mg/mL), contact time (5–180 min), pH of the solution (2.0–8.0), and the adsorbent dosage (1.0–3.5 g/L) were analyzed for their impact on the dye adsorption process. The batch experiments were studied to evaluate the influence of different operational variables such as pH, adsorbent dosage, contact time, and initial concentration of dye and were found optimum at 2, 2 g/L, 120 min, and 200 ppm, respectively, for maximum dye removal (98.33%) at ambient temperature (298 K). The isotherm models demonstrated that dye molecules were adsorbed heterogeneously in multilayer following the Freundlich isotherm ($R^2 = 0.9300$). The data were fitted for pseudo-second-order kinetics. Thus, *L. rohita* fishbone could be used as a bio-adsorbent to remove anionic dye from tannery effluents at a minimal cost.

Key words: bio-adsorbent, bio-waste, dye removal, fishbone powder, low-cost adsorbent, pollution reduction

HIGHLIGHTS

- The fishbone powder (FBP) adsorbent was prepared and characterized.
- The anionic dye removal efficiency of FBP from tannery effluent was 98.33%.
- The pH, dosage, contact time, and initial concentration of dye were optimized.
- Freundlich isotherm and pseudo-second-order kinetic model were followed.

GRAPHICAL ABSTRACT

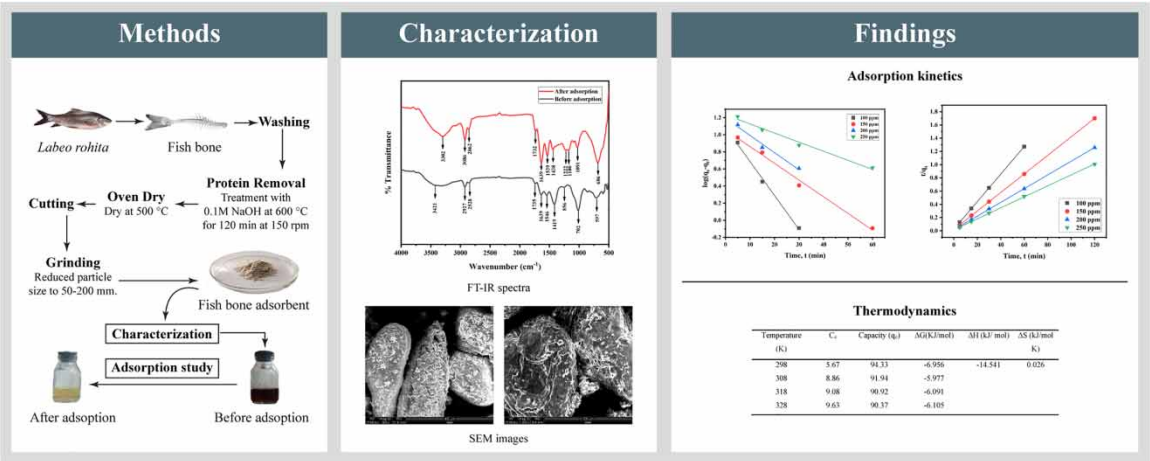

1. INTRODUCTION

The tanning process consists of several distinct chemical and physical steps, including pre-tanning, tanning, post-tanning, and finishing. After the leather has been tanned, it is then subjected to dyeing to impart various colours to the leather surface. During leather manufacturing, major discharge comes from the tanning process as chrome liquor and dyeing process containing different types of dyes, such as anionic, cationic, azo, and metal complex dyes, which reduces the water qualities. These heavy metals from spent liquor and metal complex dye contaminate not only waterbodies but also soil, and pose health risks due to the heavy metal accumulation in animals, plants, or vegetables (Ahmed *et al.* 2022a). In the leather dyeing process, a wide range of dyes are utilized, and approximately 30–40% of these dyes are wasted, which are discharged as effluent into the aquatic environment. Around 70,000 metric tons of commercial colourants are released into wastewater globally each year, as per estimation (Auta & Hameed 2011; Nassar *et al.* 2012). Different types of adsorbents are developed to reduce the chrome content in the spent liquor (Ahmed *et al.* 2022b; Tuj-Zohra *et al.* 2022) and dye from the discharged effluent. Melioderm HF (High Fastness) Brown G is mainly a homogeneous anionic dyestuff. It is most often used in leather manufacturing since it provides unique colouring and fastness capabilities for all types of leather and is thus widely employed in the leather industry. During the manufacturing of leather, some of these dyes are inevitably wasted, which results in the production of coloured effluent. Since synthetic dyes are poisonous, carcinogenic, and mutagenic, even releasing a trace amount into natural aquatic streams may have an impact on aquatic and human life (Laasri *et al.* 2007; Duman *et al.* 2016). Moreover, most dyes are resistant to deterioration by light, biological breakdown, and oxidation (Ramakrishna & Viraraghavan 1997). Therefore, proper treatment is required before releasing them into the surrounding environment. Even better approaches such as the use of non-toxic eco-friendly natural dyes extracted from natural plants, flowers, and bark instead of azo dyes (Mahdi *et al.* 2021) can reduce the pollution load.

Dye removal from aquatic environments may be accomplished in a variety of ways at present, including through the application of physical and chemical processes, biological processes, electrical and electromagnetic processes, and nuclear treatments. The processes of adsorption, ion exchange, and reverse osmosis are all examples of physicochemical processes. Meanwhile, biological processes include the reduction of microorganisms, along with aerobic and anaerobic treatment, as well as bacterial treatment (Gupta *et al.* 2009). In recent years, commercial activated carbons have gained greater popularity due to their high efficiency in dye removal from wastewater using adsorption. However, the expensive price of such adsorbent has led researchers to seek cheaper alternatives. Researchers are now pursuing several attempts to produce cost-effective adsorbents as an alternative to using instead of commercially available activated carbons. Flocculation and coagulation (Liang *et al.* 2014), oxidation (Benjelloun *et al.* 2016), and adsorption (Aguiar *et al.* 2016) are just a few of the numerous initiatives in this field. However, the majority of these approaches have serious drawbacks, such as high reagent and power requirements, low selectivity, steep operating costs, and the creation of undesirable by-products (Senturk *et al.* 2010). However, adsorption is still one of the most useful methods since it is effective, easy to implement, and relatively cheap, and there is a large variety of adsorbents to choose from (Sharma & Bhattacharyya 2005). Adsorbents for removing dyes from aqueous solutions were described in several studies, some of which are included in Table 5. Recently, Crini published a comprehensive literature review on the use of adsorbent for dye removal (Crini 2006). Furthermore, rather than discarding fishbones, which have no economic value and emit an unpleasant odour into the environment, fish wastes and leather wastewater can be managed collaboratively by using fishbone powder (FBP) as a bio-sorbent, eliminating the need for wasteful fishbone disposal. Scales from several fishes have been utilized as adsorbents in recent literature to remove anionic dyes. A recent study on the removal powder dye efficiency on two different reactive dyes, which include reactive red 2 (Begum & Kabir 2013) and reactive orange 16 (Marrakchi *et al.* 2017a), have been investigated using the bio-adsorbent derived from *Labeo rohita* fish scales. Scales of *Oreochromis niloticus* (Nile tilapia), and *Leporinus elongatus* were also used as bio-adsorbents for the removal of reactive blue 5G (Ribeiro *et al.* 2015; Neves *et al.* 2017) and remazol (yellow, blue, and red) (Vieira *et al.* 2012), respectively. There was also an attempt made to use the fish scale adsorbent to remove the cationic basic dyes, such as methylene blue dyes; nevertheless, the results were not very promising (Marrakchi *et al.* 2017b). Though multiple types of research have been carried out with fish scales, no research has been carried out using fishbone as an adsorbent, which generates a large amount of waste from the fish processing industries.

The goal of this research was to examine the feasibility of utilizing *L. rohita* FBP as a novel, uncommon, and commercially cost-effective adsorbent for the removal of Melioderm HF (High Fastness) Brown G (MHFB) dye from tannery wastewater. The organic protein collagen found in FBP is mainly accountable for the protein's capacity to absorb anionic dyes. Hydroxyapatite, an inorganic mineral, also contributes to the adsorption process (Kunkun *et al.* 2013). When it comes to dyeing wool, leather, and synthetic polyamide textiles like nylon, acid dyes are among the most popular options (Ogawa *et al.* 2004). As mentioned earlier, fishbone consists of collagen, which contains different cationic derivatives such as amide I, amide II, and amide A (Ogawa *et al.* 2004), which, as a result of their strong affinity for the anionic component of acid dyes, could have the potential to play a substantial role in the process of dye absorption. The purpose of this study was to evaluate the efficacy of FBP of *L. rohita* as a bio-adsorbent by treating fishbone with sodium hydroxide (NaOH) and then, after drying, grinding it to make powder for the removal of acid dye.

2. MATERIALS AND METHOD

2.1. Raw materials, dyes, and reagents

At first, fishbone was brought from the local market of Hazaribagh, Dhaka. During the research, MHFB was utilized as a source of reagents, which were considered model pollutants. MHFB (purity of 95.0%, a molecular weight of 342.2 g/mol, λ_{max} 443 nm) was bought from STAHL, which is a Dutch-based leather chemical manufacturing company. This dye was selected because it is most commonly used in leather industries. As a result, there is a significant opportunity for the widespread discharge of these dyes into effluents.

2.2. Preparation and characterization of adsorbent

The collected fishbones were washed to clean the filthy contaminant. Washing was carried out several times with hot distilled water. Then 0.1M sodium hydroxide (NaOH) was added to the fishbone and stirred at 150 rpm for 120 min at 60 °C to eliminate all non-fibrous protein, fat, and other impurities attached to the fishbone. Then, the fishbone adsorbent was dried at 50 °C in the oven. The adsorbent was then ground using a mechanical grinder to reduce its particle size and sieved to get a particle size of 50–200 mm (Figure 1). Following the grinding process, the adsorbents were stored in plastic bags that could keep air out.

Figure 1 | *Labeo rohita* fishbone powder.

2.3. Dye solution preparation

To prepare a stock solution with a concentration of 1,000 mg/L, 1 g of the adsorbate (MHFB dye) was dissolved in 1,000 mL of deionized water. Additionally, deionized water was used appropriately to dilute the stock solution for all subsequent experimental solutions.

2.4. Analytical methods

The sample was filtered through Whatman filter paper and the resulting supernatant was analyzed with a single-beam UV-vis spectrophotometer (VARIAN-Cary 50) at the maximum absorption wavelength ($\lambda_{max} = 443$ nm); known concentrations of the standard MHFB dye solution were used to generate a calibration curve.

2.5. Batch adsorption experiments

The adsorption experiments were all conducted in a batch procedure utilizing a thermostatically controlled agitator (IN-SK100) revolving at 150 rpm in a batch process. Dye removal of MHFB was achieved by batch adsorption onto FBP. For the adsorption equilibrium tests, a fixed quantity of adsorbent (2.0 g/L) was added to a series of 200 mL stoppered glass (Erlenmeyer flasks) holding a constant volume (25 mL in each case) of initial dye concentrations of 200 mg/L at varied pH values ranging from 2 to 8. Before reaching equilibrium, the flasks were shaken for 180 min at 150 rpm and 298 K in a temperature-controlled orbital shaker. The pH was adjusted with 0.1 N NaOH and 0.1 N hydrochloric acid solutions and measured by using a pH meter (PHS-25CW, Shanghai). At predetermined time intervals, the flasks were removed from the incubator, and the Brown G dye concentrations were measured using a single-beam UV-Vis spectrophotometer. Adsorption capacity q_e was determined by the following Equation (1):

$$q_e = \frac{(C_o - C_e)V}{W} \tag{1}$$

Here, the initial dye concentration in the liquid phase and the equilibrium dye concentration are represented by C_o and C_e (mg/L), respectively. In this equation, V denotes the volume of the solution in litres, and W indicates the amount of dye sorbent in grams. Equation (2) is used to estimate the percentage of removal of dye (%R):

$$\%\, R = \left(\frac{C_o - C_e}{C_o}\right) \times 100 \tag{2}$$

To evaluate the impact that the quantity of FBP used has on the total amount of MHFB dye that is absorbed, a series of 250 mL stoppered glass (Erlenmeyer flasks) holding a known volume (25 mL in each flask) of a predetermined initial concentration (200 mg/L) of dye solution was shaken at room temperature with varying dosages of FBP (1, 1.5, 2, 2.5, 3, and 3.5 g/L). The batch experiment was carried out at room temperature in an orbital shaker and agitated at 150 rpm for 180 min. Dye concentrations were determined during a state of equilibrium.

In order to determine the optimal contact time for adsorption, 25 mL dye solution at a fixed concentration (100–250 ppm) was treated with 2 g/L adsorbent throughout several time intervals (5–180 min).

Similarly, for equilibrium tests, kinetic studies followed a similar approach. Moreover, the assessment of dye concentrations involved the collection of aqueous samples at regular time intervals under ambient temperature. The sorption rate q_t (mg/g) was determined by Equation (3):

$$q_t = \frac{(C_o - C_t)V}{W} \tag{3}$$

The concentration of the dye in the liquid phase at a specific time is denoted by the symbol C_t (mg/L).

2.6. Kinetic models

Adsorption kinetics describes the rate at which a solid or liquid absorbs an adsorbate, as indicated by the duration of time the adsorbate spends at the interface between the solid and liquid. The analysis of dye adsorption data incorporated the utilization of the widely accepted models, namely pseudo-first-order (PFO) and pseudo-second-order (PSO) kinetics. For initial dye concentration C_o, the concentration of 100, 150, 200, and 250 mg/L were used to determine the time the reaction took and the amount of dye adsorbed. In Equation (4), the kinetic model PFO (Lagergren 1898), and in Equation (5), the kinetic model PSO (Ho & Mckay 1998) were employed to depict the adsorption of MHFB dye onto FBP:

$$\log(q_e - q_t) = \log q_e - \frac{k_1}{2.303} t \tag{4}$$

$$\frac{t}{q_t} = \frac{1}{k_2 q_e^2} + \frac{t}{q_e} \tag{5}$$

where q_e (mg/g) and q_t (mg/g) represent the dye adsorption capacity at equilibrium and at time t, respectively. Both the PFO and PSO constants may be written as k_1 (1/min) for the former and k_2 (g·mg^{-1}min^{-1}) for the latter. The initial adsorption rate may be determined with the use of the formula $h = k_2 q_e^2$. Based on the slopes of the curves and intercept of the two models, the kinetic constants and correlation coefficients were obtained.

2.7. Isotherm analysis

The equilibrium statistics are important prerequisites for the design of an adsorption system. Under the given circumstances, these statistics reveal the adsorbent's capacity to remove a certain amount of adsorbate. Adsorption equilibrium physiologies have been interpreted using Langmuir and Freundlich isotherms. To derive the isotherm constants, linear regression is often employed for model evaluation, and the least squares technique has been mostly abandoned (Cecen & Aktaş 2011; Liu *et al.* 2011; Hariani *et al.* 2013).

Among different isotherm models, the most well-known Langmuir and Freundlich models were chosen for this study because of their clarity and consistency. Adsorption of MHFB dye onto FBP was represented using the standard equilibrium models of Langmuir and Freundlich.

2.7.1. Langmuir isotherm

The Langmuir isotherm suggests that the highest level of adsorption occurs when the adsorbate is completely occupied by a single layer. Adsorption, as described by the Langmuir model, takes place at specific homogeneous sites inside the adsorbent, where the adsorbed species remain separate from one another. The following Equation (6) is the mathematical representation of the Langmuir isotherm model (Langmuir 1918):

$$\frac{q_e}{q_m} = \frac{k_L C_e}{1 + k_L C_e} \tag{6}$$

where k_L (L.m/g) is the Langmuir isotherm constant associated with the heat of adsorption, and C_e (mg/L) is the concentration of dye at equilibrium; dye adsorption equilibrium quantity (q_e) and maximum monolayer adsorption capacity (q_m) are both expressed as milligrams per gram (mg/g). The Langmuir isotherm can be expressed in linear form as in Equation (7):

$$\frac{C_e}{q_e} = \frac{1}{k_L q_m} + C_e \frac{1}{q_m} \tag{7}$$

Adsorption may be shown to follow the Langmuir model, as seen by the linear relationship between $1/q_e$ and $1/C_e$, where q_m and k_L can be determined by using the intercept and slope of this line. The equilibrium parameter, R_L, is dimensionless and defines the Langmuir isotherm, as seen in the following equation:

$$R_L = \frac{1}{1 + kC_o} \tag{8}$$

where C_o (mg/L) is the initial concentration of dye. Values of R_L indicate the degree of adsorption as follows:

- If $0 > R_L > 1$, then adsorption is favourable.
- If $R_L > 1$, unfavourable adsorption will occur.
- If $R_L = 1$, adsorption is linear.
- If $R_L = 0$, then adsorption is irreversible.

2.7.2. Freundlich isotherm

In the Freundlich isotherm model, adsorption is considered to take place on a heterogeneous surface in several layers and to include molecular interaction. The model is expressed as follows:

$$q_e = k_F C_e^{\frac{1}{n}} \tag{9}$$

The Freundlich constant, k_F ((mg/g) (L/mg)$^{1/n}$), coupled with a heterogeneity factor, indicates the adsorption capacity, whereas the empirical parameter, n, determines the favourability. To achieve optimal adsorption

conditions, 'n' must be greater than 1. The linear form of the Freundlich model is:

$$\ln q_e = \ln k_F + \frac{1}{n} \ln C_e \tag{10}$$

The Freundlich constants k_F and n were determined from the linear plot of ln q_e vs ln C_e.

2.8. Adsorption thermodynamics

Studies in thermodynamics were carried out, and the characteristics and fundamental processes of the adsorption reactions were investigated and validated. The Gibbs free energy (ΔG), enthalpy (ΔH), and change in standard entropy (ΔS) are all examples of thermodynamic parameters (Ponnusamy & Gayathri 2009). These parameters are a true measure of how well the dye adsorption procedure will work in real life. In the dye adsorption procedure, the value of the parameter ΔG indicates whether or not the reaction has spontaneously occurred; similarly, dye adsorption reactions may be characterized as either endothermic reaction or exothermic, depending on the value of ΔH, and the value of ΔS during the adsorption of dye to a solid or liquid surface reflects the level of disorder present at the solid–liquid interface.

The thermodynamics parameters were determined by Equations (11)–(13) (Liu 2009; Zhou *et al.* 2012; Ausavasukhi *et al.* 2016):

$$k_d = \frac{q_e}{C_e} \tag{11}$$

$$\ln K_d = \frac{\Delta S}{R} - \frac{\Delta H}{RT} \tag{12}$$

$$\Delta G = \Delta H - T\Delta S \tag{13}$$

where, k_d = distribution coefficient of adsorption (q_e/c_e), R = universal gas constant (8.314 $Jmol^{-1}K^{-1}$), and T = temperature (K).

3. RESULTS AND DISCUSSION

3.1. Adsorbent characterization

3.1.1. Spectral analysis

Fourier-transform infrared spectroscopy (FTIR) was used to identify the functional groups present on the surface of FBP. Developing adsorption behaviours, especially for chemisorption, requires identifying functional groups as a primary concern. Figure 2 illustrates the FTIR spectrum of FBP before and after MHFB dye adsorption. The variation in absorption peaks was observed and given in Table 1.

The N-H stretching mode of amide A displays a relatively wide and elevated shape reminiscent of a mountain, with the peak positioned approximately at 3302 and 3421 cm^{-1}. The success of dye removal relied on the surface properties of the prepared adsorbent, underscoring their crucial role in the adsorption process. To find out the particular functional groups accountable for anionic dye adsorption, FTIR was used in the range of 4,000–400 cm^{-1}. Fishbone has characteristic amide I, amide II, amide III, OH bond, amide B, and acid group, which were confirmed by FTIR peaks of 1,639, 1,419, 1,253, 3,421, 2,927, and 2,528 cm^{-1}, respectively. Stretching vibrations of carbonyl groups (C = O bond) were primarily responsible for the presence of the amide I band, with typical frequencies in the range of 1,600–1,700 cm^{-1} (Payne & Veis 1988). It has been revealed that the location of the amide II bands has changed to a lower frequency, 1,419 cm^{-1}, indicating the presence of H-bonding in each collagen molecule.

The O–H stretching mode of alcohols displays a relatively wide and elevated shape reminiscent of a mountain, with the peak positioned approximately at 3,400 cm^{-1}. The hydrogen bonds that existed between different molecules were responsible for the propagation of this signal. The peak found between 2,900 and 3,000 cm^{-1} indicated the presence of amide B having CH_2 asymmetrical vibration. The peak at 1,735 cm^{-1} suggested that C = O bonds were present (Chandrajith & Marapana 2018). Fishbone-derived collagen exhibits characteristics similar to type I collagen, comprising two $\alpha 1$ chains and one $\alpha 2$ chain (Kimura *et al.* 1991; Yunoki *et al.* 2003). Fishbone is comprised of collagen and consists of different types of amides (amide I, amide II, and amide II) having NH_2 and NH groups. According to the study of Nawi *et al.* (2010), these groups are protonated

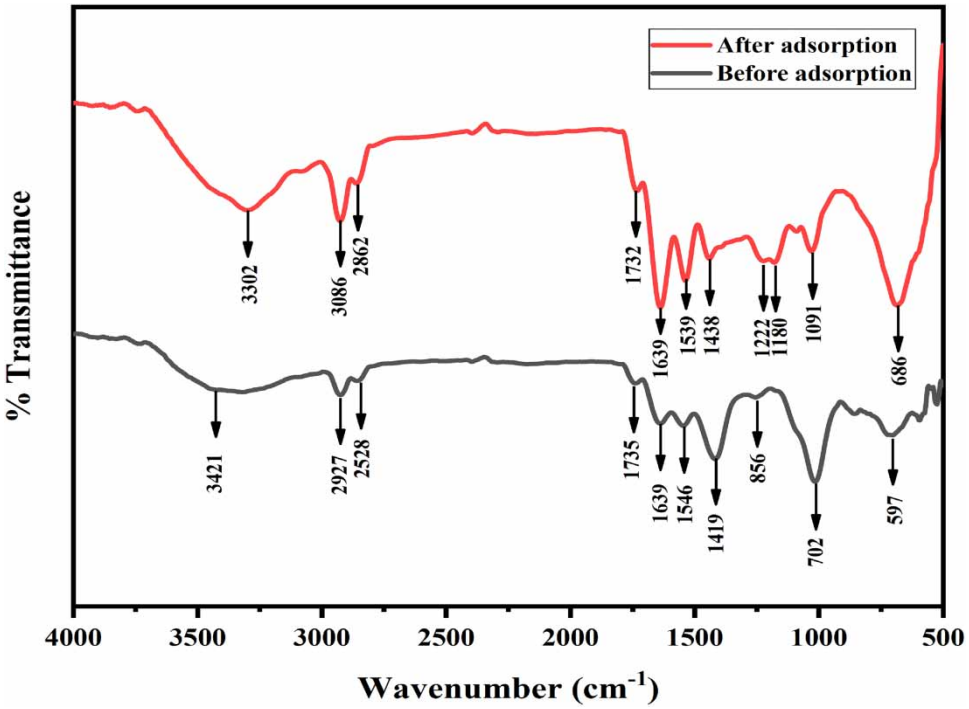

Figure 2 | FTIR spectra of FBP before and after dye adsorption.

Table 1 | Absorption peaks of FBP adsorbent before and after dye adsorption

Before adsorption			After adsorption			
Main functional groups	**Peaks (cm^{-1})**	**Corresponding vibrations**	**Main functional groups**	**Peaks (cm^{-1})**	**Corresponding vibrations**	**References**
Amide I	1,639	Stretching vibrations C = O	Amide I	1,639	C–O stretching vibration	Payne & Veis (1988)
Amide II	1,419	C–H stretching and N–H bending	Amide II	1,434	C–H stretching and N–H bending	Jackson *et al.* (1995)
Amide III	1,253	NH bending coupled with CN stretching	Amide III	1,222 1,180	N–H bending coupled with C–N stretching	Payne & Veis (1988)
Amide A	3,421	N-H stretching	Amide A	3,302	N–H stretching	Ji *et al.* (2020)
Amide B	2,927	CH_2 asymmetrical stretching	Amide B	2,927	CH_2 asymmetrical stretching	Abe & Krimm (1972)
Acid groups	2,528	OH group	Alkane	2,862	CH_3 stretching vibration	Do *et al.* (2013), Dobos *et al.* (2012)

as NH^{3+}. Negatively charged anionic dye molecules are fixed with positively charged amide groups of adsorbents via hydrogen bonding during adsorption.

3.1.2. SEM analysis

SEM was subjected to study the apparent morphology of the adsorbent before and after applying dye. The SEM photographs depicted in Figure 3, captured at magnifications of 500× and an acceleration voltage of 15 kV, illustrate the availability of pores on both the adsorbent and its internal surfaces. Images presented in Figure 4, captured at 500 and 1,000× magnification, showcase the surface porosity and pore structures following dye adsorption. These images reveal a decrease in porosity and the formation of a dye layer on the adsorbent's surface, supporting the effective adsorption capability of FBP.

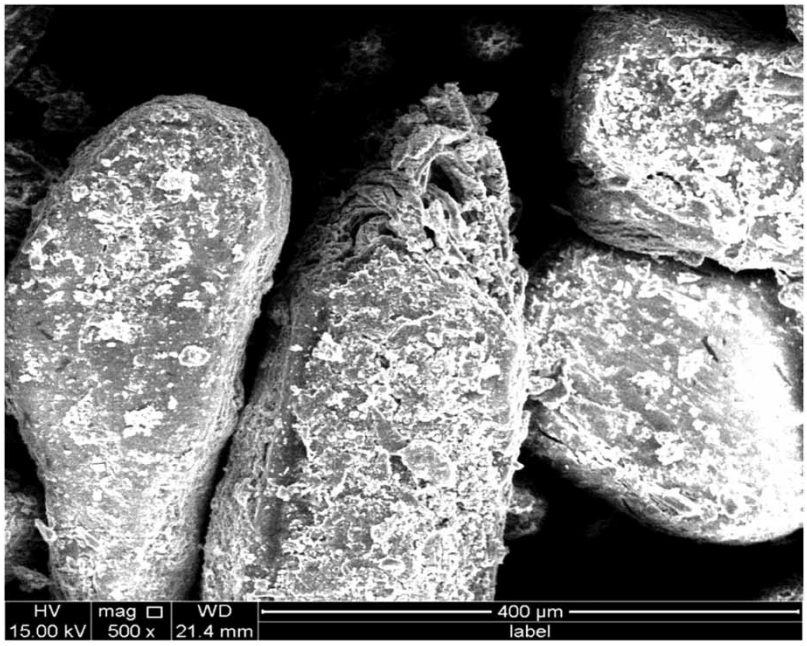

Figure 3 | SEM images at 500× magnification of FBP before dye adsorption.

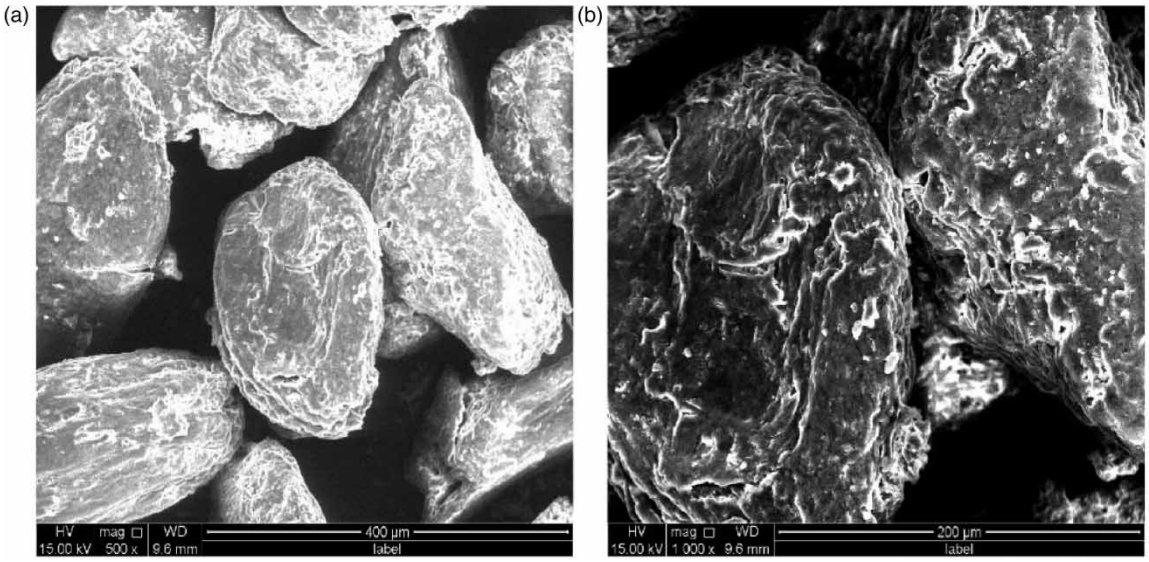

Figure 4 | SEM images at (a) 500× and (b) 1,000× magnification of FBP after dye adsorption.

3.2. Effect of pH on dye adsorption

Experiments were carried out using an initial MHFB dye concentration of 200 mg/L, an FBP dosage of 0.20 g/L, and a temperature of 298 K to examine the impact of solution pH on the equilibrium absorption capacity of the adsorbent. In Figure 5, the impact of pH on dye removal by FBP adsorbent was investigated by subjecting the dye solution to varying pH ranges (2–8). The figure demonstrates that a decrease in pH from 8.0 to 2.0 led to a substantial improvement in MHFB removal, with the removal percentage rising from 38.65 to 98.33%. At a pH of 2, MHFB sorption was at its highest. The percentage of removal was dramatically reduced, with only a little rise in pH value from 2 to 3. The adsorbent's ability to remove dye gradually reduced after pH 3, reaching a minimum at a level of pH 7. Consequently, pH 2 was selected as the optimum pH for dye adsorption.

In polyamides (collagen), the NH_2 and NH groups were responsible for the compound's high sensitivity to pH, as these groups were protonated as NH^{3+} at a pH of 2.0 (Nawi *et al.* 2010). The presence of a higher number of

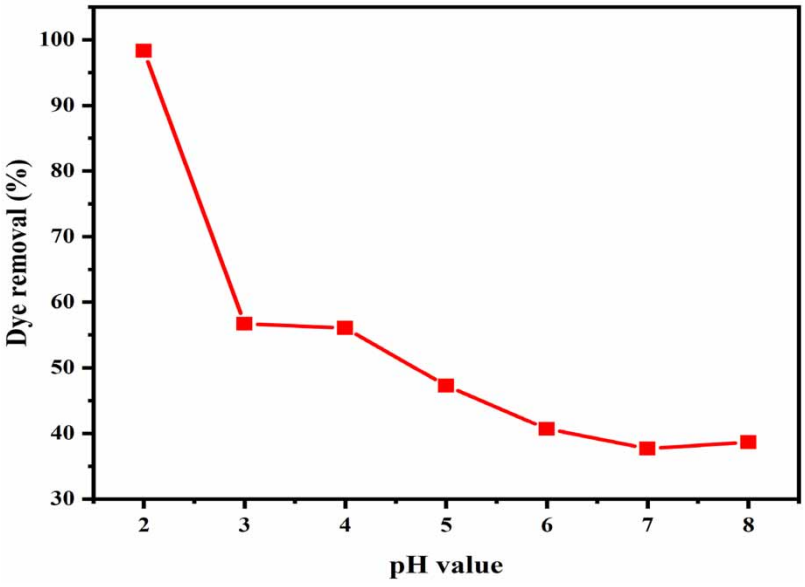

Figure 5 | Effect of pH on MHFB adsorption.

protons at a low pH of 2.0 leads to a substantial increase in adsorption capacities, promoting the effective uptake of the anionic dye:

$$\text{Dye} - SO_3Na \xrightarrow{\text{At lower pH}} \text{Dye} - SO_3H$$

$$\text{Dye} - SO_3H \underset{\text{Lower pH}}{\overset{\text{Higher pH}}{\rightleftharpoons}} \text{Dye} - SO_3^-$$

A synergistic and beneficial effect for adsorption might be provided by the attraction of the negatively charged dye molecules and the repulsion between the positively charged polymeric chains of collagen caused by the protonated amino groups. Both of these factors contributed to the positive charge on the collagen chains. A previous study discovered a pattern that was quite similar to this one when they absorbed RB19 dye onto hollow chitosan nanofibers (Mirmohseni *et al.* 2012). They were able to demonstrate an increase in adsorption capacity by bringing the initial pH of the solution down from 7.5 to 3.5. An analogous research endeavour involved using fish scales as a bio-adsorbent to effectively eliminate anionic acid dyes (acid red 1, acid blue 45, and acid yellow 127) present in the wastewater produced during textile dyeing operations (Kabir *et al.* 2019). The investigation of the FTIR peaks revealed that the primary facilitators in the reaction with anionic dyes (sodium salts of sulfonic acid dyes) were polypeptide (amide) groups derived from polymer chain amino acids (amide A, amide I, and amide II).

3.3. Effect of adsorbent dosage on dye adsorption

The research aimed to examine the elimination of MHFB dye by treating effluent samples with known concentrations to different dosages of adsorbent under optimal pH conditions. To investigate the influence of adsorbent dosage on dye adsorption, experiments were carried out using an initial MHFB concentration of 200 mg/L (Figure 6).

The adsorption studies indicated a continuous rise in the MHFB removal proportion up to 2 g/L of adsorbent dosage. However, after reaching its maximum at 3 g/L, further increases in the dosage had no additional effect on dye removal, maintaining a stable removal percentage. It was found that the maximum adsorption capacity was achieved for a 2 g/L dosage, and the capacity was progressively reduced with an increasing amount of adsorbent. As a result, the experiment showed that 2 g/L was the optimum dosage concentration.

3.4. Effect of contact time and initial concentration

The correlation between contact time and dye removal was determined by treating a 25 mL dye solution with a fixed concentration (100–250 ppm) using 2 g/L of adsorbent at specific time intervals (5–180 min) under the optimal pH conditions. The outcomes are presented in Figure 7.

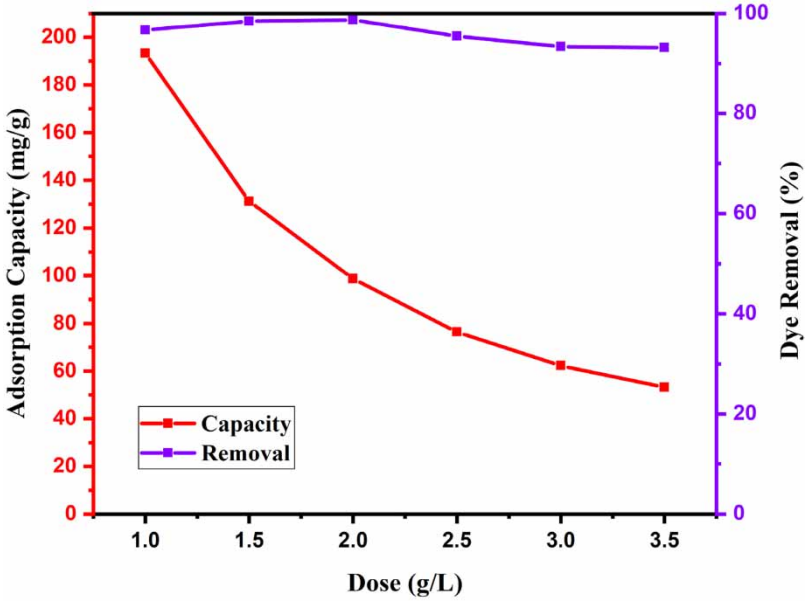

Figure 6 | Effect of adsorbent dosage on the adsorption of MHFB dye on FBP.

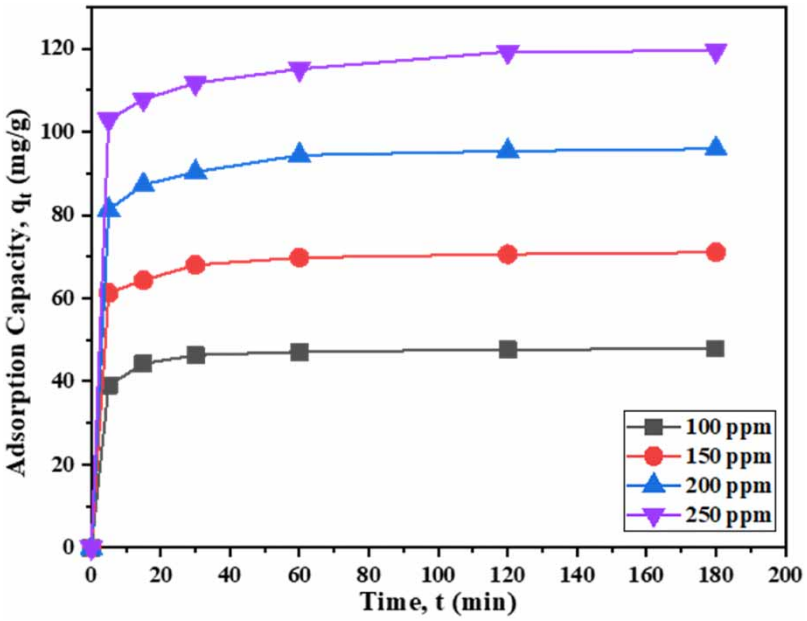

Figure 7 | Contact time and initial concentration effect on dye adsorption onto FBP adsorbent.

The plots can be divided into three distinct stages: (1) the immediate adsorption that takes place within the first 15 min, (2) the gradual movement towards equilibrium until reaching the equilibrium point for each concentration, and (3) the equilibrium state. Dye removal from the water sample was shown to be dosage-dependent, with longer contact times resulting in a greater reduction in dye concentration, until a point when the adsorption rate became negligible after 120 min. For that reason, the optimum contact time was 120 min for this adsorption study. The data showed that the adsorption of MHFB dye onto FBP was increased with increasing initial MHFB dye concentration. To ensure that complete equilibrium had been reached, the experiment was run for 180 min, and the experimental results were collected.

These findings were consistent with the notion that dye molecules must first interact with the boundary layer, and then molecules enter the adsorbent surface by diffusing from the boundary layer film. Afterwards, they must

enter the adsorbent's porous matrix through diffusion (Senthilkumaar *et al.* 2005; Faust & Aly 2018). Since there were more dye molecules in higher initial concentrations of MHFB solutions, it took more time for them to reach equilibrium. Maximum adsorption capabilities were also seen in all dosages at greater initial concentrations. Increasing the initial MHFB dye concentration from 100 to 250 mg/L influenced the adsorption capacity, which went from 47.66 to 119.22 mg/g at equilibrium.

3.5. Isotherm analysis

Experiments were conducted in batches with MHFB dosages ranging from 100 to 250 mg/L. Factors influencing the adsorption process were kept constant throughout the operation (2.0 g/L FBP dosage, 200 rpm shaker speed, a 25.0 mL solution volume, and a temperature of 298 K).

The Langmuir and Freundlich isotherms were used to do the statistical analysis of the outcomes of the equilibrium isotherms. Figures 8 and 9 illustrate the Langmuir and Freundlich isotherm model of MHFB adsorption onto FBP, respectively.

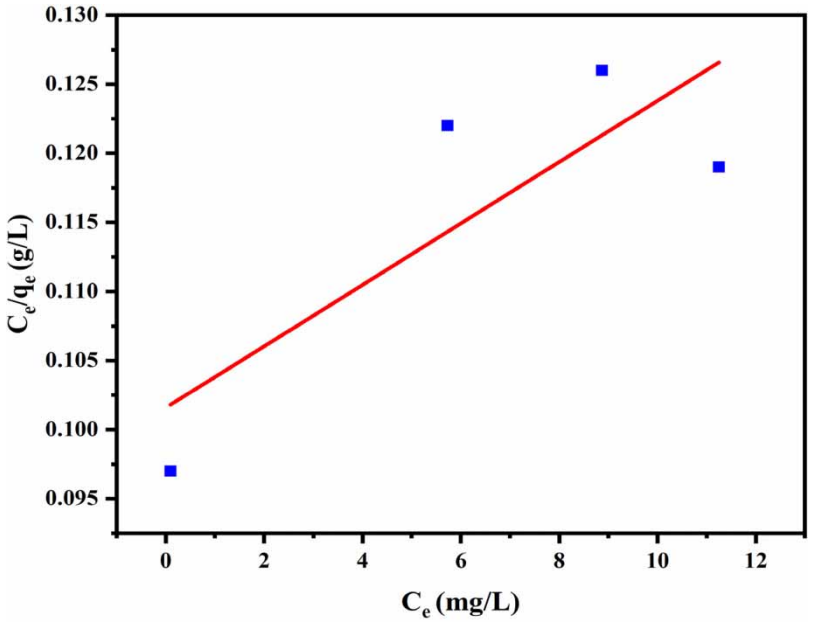

Figure 8 | Langmuir isotherm model of MHFB adsorption onto FBP.

The calculated values for the Langmuir and Freundlich parameters, as well as the R^2 values (which were obtained from the non-linear regression analysis), are presented in Table 2. The findings of this study revealed that the Freundlich isotherm model offered a superior fit for the dye adsorption process compared to the Langmuir model. This observation indicates that the adsorption of dye onto FBP involves heterogeneous multilayer adsorption.

3.6. Adsorption kinetics

The experimental data used to describe the sorption mechanism and identify the rate-limiting phase were represented in the field of sorption kinetics. Similar to isothermal studies, kinematics feasibility can be estimated with a linear plot of reaction models and an estimate of the regression coefficient (R^2). The kinetics were evaluated by introducing 2 g/L of adsorbent at pH 2 and conducting the adsorption test for a predetermined period and concentration of dye (100–250 ppm).

To establish the rate parameters, the straight-line plots of log ($q_e - q_t$) against time (Figure 10) for the adsorption of MHFB onto FBP were also subjected to testing. Table 3 displays the results of these plots in terms of the k_1, k_2, $q_e{}^a$, and corresponding R^2 under varying MHFB concentrations. The regression coefficient, R^2, values for the first-order kinetic model were greater than or equal to 0.981. Plots of t/q_t against t for second-order kinetics are shown in Figure 11. For all dosages tested, the PSO model had R^2 values greater than or equal to 0.999, which were much greater than those of the PFO model. Moreover, the experimental $q_e{}^a$ of PFO did not match the

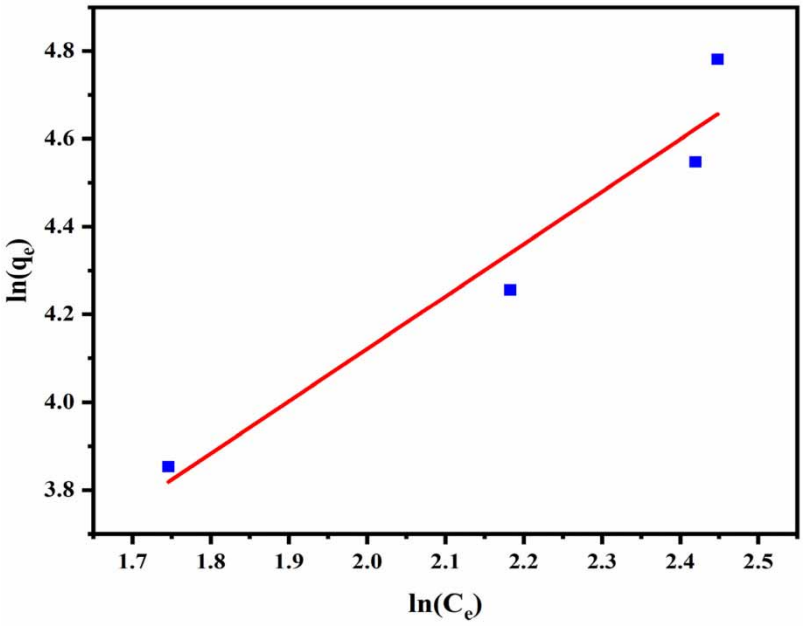

Figure 9 | Freundlich isotherm model of MHFB adsorption onto FBP.

Table 2 | Isotherm parameters for MHFB dye removal by FBP

Isotherms	Parameters	Value
Langmuir	k_L (L/mg)	0.0214
	R^2	0.6800
	R_L	0.1550
Freundlich	k_F ((mg/g) (L/mg)$^{(1/n)}$)	5.6670
	n	0.8379
	R^2	0.9300

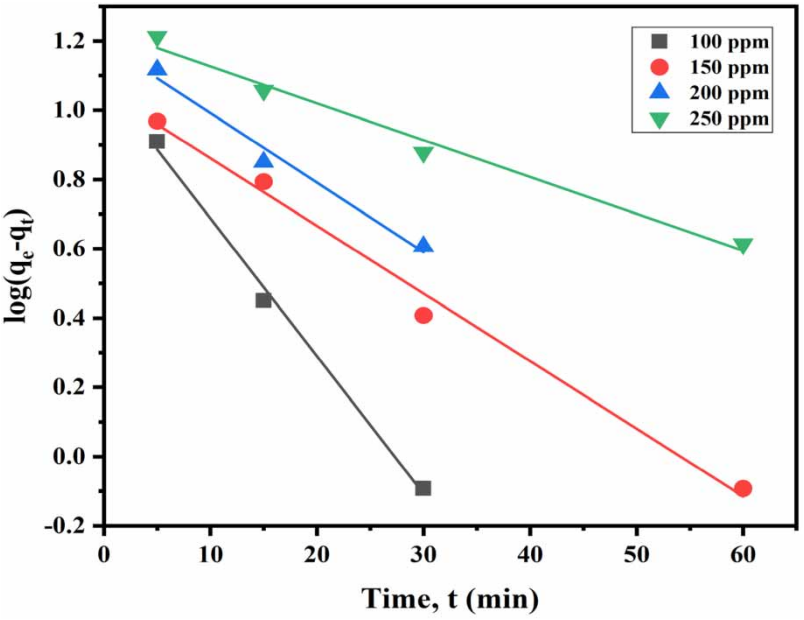

Figure 10 | Pseudo-first-order reaction models for dye adsorption onto fishbone adsorbent.

Table 3 | Summary of adsorption studies

Kinetics model	Parameters	100 mg L^{-1}	150 mg L^{-1}	200 mg L^{-1}	250 mg L^{-1}
Pseudo-first-order (PFO)	q_e[a] (mg g^{-1})	47.14	70.56	95.35	119.22
	k_1	0.0916	0.049	0.0462	0.0245
	R^2	0.995	0.991	0.981	0.985
	q_e[b] (mg g^{-1})	12.175	11.4	15.59	17.10
Pseudo-second-order (PSO)	q_e[a] (mg g^{-1})	47.14	70.56	95.35	119.22
	k_2	0.0175	0.01127	0.00733	0.00477
	R^2	1.000	0.999	0.999	0.999
	q_e[b] (mg g^{-1})	48.07	71.28	96.43	120.48

[a]Experimental.
[b]Theoretical.

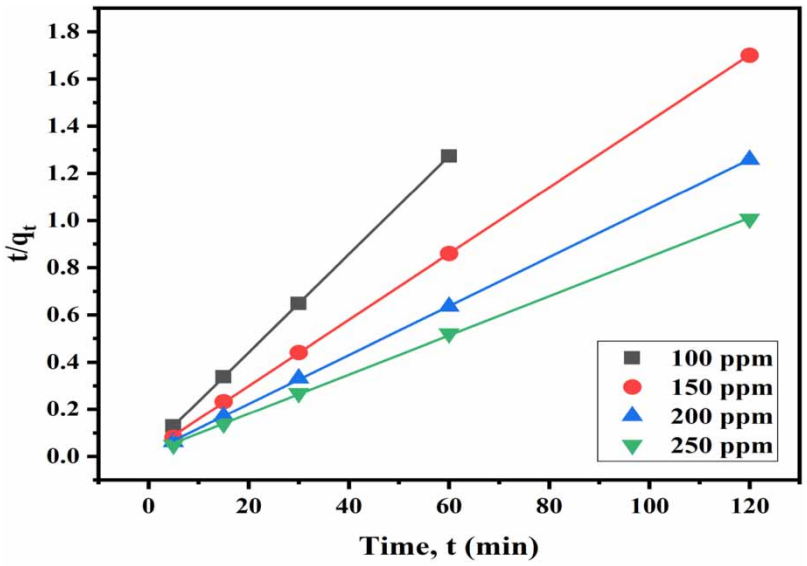

Figure 11 | Pseudo-second-order reaction models for dye adsorption onto fishbone adsorbent.

theoretical q_e[b], and the values of q_e[b] were quite similar to q_e[a] in the case of the PSO kinetic model. This research revealed that the production of chemical bonds between the adsorbent and the adsorbate throughout the adsorption process was the principal adsorption mechanism and that the PSO model was the more relevant (Hubbe *et al.* 2019). In addition, the dye adsorption process was two-staged, with the first stage being the dissociation of dye ion complexes and the second stage being the binding of these ions to the surface of the adsorbent's functional groups i.e. active sites (Robati 2013). Adsorption of MHFB onto FBP proceeded according to a PSO kinetics model, i.e. the chemisorption adsorption process.

3.7. Adsorption thermodynamic results

The changes in thermodynamic parameters such as Gibbs free energy (ΔG), enthalpy (ΔH), and standard entropy (ΔS) as a result of the dye's presence are the most significant. Adsorption thermodynamics were analyzed using the typical values for entropy (ΔG, ΔH, and ΔS). Table 4 displays the findings.

Table 4 | Study of thermodynamic parameters for dye adsorption onto FBP adsorbent

Temperature (K)	C_e	Capacity (q_e)	ΔG (kJ/mole)	ΔH (kJ/ mole)	ΔS (kJ/mole K)
298	5.67	94.33	−6.956	− 14.541	0.026
308	8.86	91.94	−5.977		
318	9.08	90.92	−6.091		
328	9.63	90.37	−6.105		

The negative ΔG values suggested that the adsorption of both dyes occurred spontaneously and favourably. At a temperature of 298 K, more negative ΔG values were discovered; this finding provided more evidence that adsorption was preferred at this temperature. The positive ΔS values (0.026 kJ/mole) indicated that some rearrangements on the solid–liquid interface had been placed throughout the adsorption process. Additionally, these values also showed how the adsorption of MHFB dye onto FBP adsorbent led to a lessening of haphazardness at the solid solution interface. The negative values of enthalpy ($\Delta H = -14.541$ kJ/mole < 0) verify the exothermic nature of dye adsorption.

During adsorption, molecules of the adsorbate are attracted to the adsorbent's surface. The heat of adsorption is negative, indicating that energy is continually being released throughout the adsorption process, making it exothermic. Due to the magnitude of ΔH, it was determined that physical interactions were involved in the

Table 5 | Efficiency of fishbone powder adsorbent in comparison to other bio-adsorbents

Bio-adsorbent	Dye investigated	Max. adsorption capacities (mg/g)	Reference
Labeo rohita scales	MG	38.46	Chowdhury *et al.* (2012)
Tamarind fruit shell	MG	1.951	Saha *et al.* (2010)
Bentonite	MG	7.72	Tahir & Rauf (2006)
Oil palm trunk fibre	MG	149.35	Hameed & El-Khaiary (2008a)
Seashell powder	MG	42.33	Chowdhury & Saha (2010)
Neem leaf powder	MG	66.72	Das *et al.* (2020)
Caulerpa racemosa var. *cylindracea*	MB	3.423	Cengiz & Cavas (2008)
Luffa cylindrica fibres	MB	47	Demir *et al.* (2008)
Grass waste	MB	457.640	Hameed (2009)
Broad bean peels	MB	192.7	Hameed & El-Khaiary (2008b)
Castor seed shell	MB	158.73	Oladoja *et al.* (2008)
Yellow passion fruit waste	MB	44.70	Pavan *et al.* (2008)
Untreated desert plant	MB	295	Bestani *et al.* (2008)
Chemically activated desert plant	MB	130	
Pyrolized desert plant	MB	53	
Watermelon (*Citrullus lanatus*) rinds	MB	115.61	Shukla *et al.* (2023)
Chitosan-pectin composite	MB	328.02	Mohrazi & Ghasemi-Fasaei (2023)
Cellulose citrate	MB	96.2	Olivito *et al.* (2021)
Composite beads of sodium alginate/halloysite/hemp hurd	MB	50	Viscusi *et al.* (2022)
$ZnCl_2$ modified (ZAB)	MO	101.43	Maiti *et al.* (2023)
Date seed	MV	59.5	Ali *et al.* (2022)
Pineapple leaf powder	BG 4	56.64	Chowdhury *et al.* (2011)
Chitosan-based adsorbent	BB 3	166.5	Crini *et al.* (2008)
Soy meal hull	DR 80 DR 81 AB 92 AR 14	178.57 120.482 114.943 109.89	Arami *et al.* (2006)
Mg $(OH)_2/Fe_3O_4$/PEI functionalized enzymatic lignin composite	CR	74.7	Zong *et al.* (2023)
Wheat flour	RB	142.26	Hasan *et al.* (2021)
L. rohita fishbone powder	Melioderm HF Brown G	119.22	This study

Note: MG, malachite green; MB, methylene blue; MO, methyl orange; MV, methyl violet; BG, basic green; BB, basic blue; DR, direct red; AB, acid blue; AR, acid red; CR, Congo red; RB, rhodamine B; PEI, Poly(ethyleneimine).

adsorption of the dye (Von Oepen *et al.* 1991). In particular, these ΔH values are indicative of the potential participation of both van der Waals and electrostatic interactions in the adsorption of the dye on the FBP (Khani *et al.* 2011; Hemmateenejad *et al.* 2015). A reduction in adsorption from 94.33 to 90.37 mg/g was observed for MHFB dye on FBP adsorbent when the temperature was raised from 298 to 328 K. Rising temperatures inhibit dye absorption, which explains the phenomenon. This is supported by the fact that the solubility of the dye decreases with increasing temperature (Dotto *et al.* 2012), which is a reflection of the increased interaction between the adsorbed dye molecules.

3.8. Comparison of fish scale with other sorbents

The maximal adsorption capabilities of a variety of bio-adsorbents, including FBP, were compared and summarized. Based on the findings of the comparison, the fish scale has a greater malachite green (MG) binding capacity than the majority of the other biosorbents that have been described. Fish scales provided several other benefits, including their simple accessibility and favourable cost structure, which pointed to a bright future for their use in the elimination of MG from aqueous solutions. It can be observed from Table 5 that *L. rohita* FBP showed higher adsorption capacity than the *L. rohita* fish scales and other bio-adsorbents such as tamarind fruit shell, bentonite, sea shell powder, *Luffa cylindrica* fibres, yellow passion fruit waste, sunflower seed hull, and pineapple leaf powder.

4. CONCLUSIONS

The results of this investigation showed that FBP, a by-product of the fish processing industry, had excellent adsorption capacity for anionic dye from aqueous solutions. Since 98.33% removal was achieved at a pH level of 2, it is clear that the adsorption mechanism is very sensitive to pH. Dye is adsorbed rapidly during the first 15 min of contact time and then at a decreasing rate until equilibrium is reached after around 120 min, as shown by the impact of contact time. Langmuir and Freundlich's isotherms were employed to analyze the equilibrium data, and the Freundlich isotherm demonstrated the strongest correlation (R^2 was extremely close to the unity), suggesting chemisorption behaviour on a heterogeneous multilayer surface. For a variety of starting MHFB concentrations, the kinetic data are highly consistent with a PSO model ($R^2 \geq 0.999$). There was an increase in order at the adsorbent–solution interface, which is consistent with the adsorption process being spontaneous, exothermic, and technically viable, as shown by the thermodynamic characteristics. The thermodynamic constants show a very low rate and indicate physisorption. Based on kinematics and thermodynamics, we can conclude the process is physicochemical adsorption. The successful synthesis of the adsorbent was confirmed through the examination of its morphology, structural properties, and elemental compositions using SEM and FTIR techniques. FTIR confirmed the presence of amide groups in the adsorbent. The morphological structure and surface of FBP adsorbent were visible with a rough surface. The SEM image indicated the changed morphology by destroying the surface with no noticeable edges and a nearly smooth surface due to chemical modifications. According to the findings of this research, the FBP derived from *L. rohita* can be employed effectively as a cost-effective adsorbent for the removal of anionic dyes from an aqueous solution.

DATA AVAILABILITY STATEMENT

All relevant data are included in the paper or its Supplementary Information.

CONFLICT OF INTEREST

The authors declare there is no conflict.

REFERENCES

Abe, Y. & Krimm, S. 1972 Normal vibrations of crystalline polyglycine I. *Biopolymers* **11**(9), 1817–1839. https://doi.org/10.1002/bip.1972.360110905.

Aguiar, J. E., de Oliveira, J. C. A., Silvino, P. F. G., Neto, J. A., Silva, I. J. & Lucena, S. M. P. 2016 Correlation between PSD and adsorption of anionic dyes with different molecular weights on activated carbon. *Colloids and Surfaces A: Physicochemical and Engineering Aspects* **496**, 125–131. https://doi.org/10.1016/j.colsurfa.2015.09.054.

Ahmed, S., Tuj-Zohra, F., Mahdi, M. M., Nurnabi, M., Alam, M. Z. & Choudhury, T. R. 2022a Health risk assessment for heavy metal accumulation in leafy vegetables grown on tannery effluent contaminated soil. *Toxicology Reports* **9**, 346–355. https://doi.org/10.1016/j.toxrep.2022.03.009.

Ahmed, S., Tuj-Zohra, F., Mahdi, M., Mahmudunnabi, D., Choudhury, T., Alam, Z. & Nurnabi, M. 2022b Synthesis and characterization of graphene oxide for removal of Cr (III) from tannery effluent. *Desalination and Water Treatment* **244**, 201–211. https://doi.org/10.5004/dwt.2021.27895.

Ali, N. S., Jabbar, N. M., Alardhi, S. M., Majdi, H. S. & Albayati, T. M. 2022 Adsorption of methyl violet dye onto a prepared bio-adsorbent from date seeds: Isotherm, kinetics, and thermodynamic studies. *Heliyon* **8**(8), e10276. https://doi.org/10.1016/j.heliyon.2022.e10276.

Arami, M., Limaee, N. Y., Mahmoodi, N. M. & Tabrizi, N. S. 2006 Equilibrium and kinetics studies for the adsorption of direct and acid dyes from aqueous solution by soy meal hull. *Journal of Hazardous Materials* **135**(1–3), 171–179. https://doi.org/10.1016/j.jhazmat.2005.11.044.

Ausavasukhi, A., Kampoosaen, C. & Kengnok, O. 2016 Adsorption characteristics of Congo red on carbonized leonardite. *Journal of Cleaner Production* **134**, 506–514. https://doi.org/10.1016/j.jclepro.2015.10.034.

Auta, M. & Hameed, B. H. 2011 Preparation of waste tea activated carbon using potassium acetate as an activating agent for adsorption of acid blue 25 dye. *Chemical Engineering Journal* **171**(2), 502–509. https://doi.org/10.1016/j.cej.2011.04.017.

Begum, H. & Kabir, M. 2013 Removal of brilliant red from aqueous solutions by adsorption on fish scales. *Dhaka University Journal of Science* **61**(1), 7–12. https://doi.org/10.3329/dujs.v61i1.15089.

Benjelloun, Y., Miyah, Y., Idrissi, M., Boumchita, S., Lahrichi, A., El Ouali Lalami, A. & Zerrouq, F. 2016 Study of catalytic performance for the oxidation of methylene blue using MnO-Clay catalyst with H_2O_2. *Journal of Materials and Environmental Science* **7**(1), 9–17.

Bestani, B., Benderdouche, N., Benstaali, B., Belhakem, M. & Addou, A. 2008 Methylene blue and iodine adsorption onto an activated desert plant. *Bioresource Technology* **99**(17), 8441–8444. https://doi.org/10.1016/j.biortech.2008.02.053.

Cecen, F. & Aktaş, Ö. 2011 *Activated Carbon for Water and Wastewater Treatment: Integration of Adsorption and Biological Treatment*. Wiley Online Library, USA. https://doi.org/10.1002/9783527639441

Cengiz, S. & Cavas, L. 2008 Removal of methylene blue by invasive marine seaweed: *Caulerpa racemosa* var. *cylindracea*. *Bioresource Technology* **99**(7), 2357–2363. https://doi.org/10.1016/j.biortech.2007.05.011.

Chandrajith, G. & Marapana, U. 2018 Physicochemical characters of bark exudates of *Lannea coromandelica* and its application as a natural fruit coating. *Journal of Pharmacognosy and Phytochemistry* **7**(4), 1798–1802.

Chowdhury, S. & Saha, P. 2010 Sea shell powder as a new adsorbent to remove Basic Green 4 (malachite green) from aqueous solutions: Equilibrium, kinetic and thermodynamic studies. *Chemical Engineering Journal* **164**(1), 168–177. https://doi.org/10.1016/j.cej.2010.08.050.

Chowdhury, S., Chakraborty, S. & Saha, P. 2011 Biosorption of basic green 4 from aqueous solution by *Ananas comosus* (pineapple) leaf powder. *Colloids and Surfaces. B, Biointerfaces* **84**(2), 520–527. https://doi.org/10.1016/j.colsurfb.2011.02.009.

Chowdhury, S., Das Saha, P. & Ghosh, U. 2012 Fish (*Labeo rohita*) scales as potential low-cost biosorbent for removal of malachite green from aqueous solutions. *Bioremediation Journal* **16**(4), 235–242. https://doi.org/10.1080/10889868.2012.731444.

Crini, G. 2006 Non-conventional low-cost adsorbents for dye removal: A review. *Bioresource Technology* **97**(9), 1061–1085. https://doi.org/10.1016/j.biortech.2005.05.001.

Crini, G., Gimbert, F., Robert, C., Martel, B., Adam, O., Morin-Crini, N., De Giorgi, F. & Badot, P.-M. 2008 The removal of basic blue 3 from aqueous solutions by chitosan-based adsorbent: Batch studies. *Journal of Hazardous Materials* **153**(1–2), 96–106. https://doi.org/10.1016/j.jhazmat.2007.08.025.

Das, R., Mukherjee, A., Sinha, I., Roy, K. & Dutta, B. K. 2020 Synthesis of potential bio-adsorbent from Indian Neem leaves (*Azadirachta indica*) and its optimization for malachite green dye removal from industrial wastes using response surface methodology: Kinetics, isotherms and thermodynamic studies. *Applied Water Science* **10**(5), 117. https://doi.org/10.1007/s13201-020-01184-5.

Demir, H., Top, A., Balköse, D. & Ülkü, S. 2008 Dye adsorption behavior of *Luffa cylindrica* fibers. *Journal of Hazardous Materials* **153**(1), 389–394. https://doi.org/10.1016/j.jhazmat.2007.08.070.

Do, B., Nguyen, B., Nguyen, H. & Nguyen, P.-T. 2013 Synthesis of magnetic composite nanoparticles enveloped in copolymers specified for scale inhibition application. *Advances in Natural Sciences: Nanoscience and Nanotechnology* **4**, 7. https://doi.org/10.1088/2043-6262/4/4/045016.

Dobos, A. M., Onofrei, M.-D., Stoica, I., Olaru, N., Olaru, L. & Ioan, S. 2012 Rheological properties and microstructures of cellulose acetate phthalate/hydroxypropyl cellulose blends. *Polymer Composites* **33**, 2072–2083. https://doi.org/10.1002/pc.22350.

Dotto, G. L., Lima, E. C. & Pinto, L. A. A. 2012 Biosorption of food dyes onto *Spirulina platensis* nanoparticles: Equilibrium isotherm and thermodynamic analysis. *Bioresource Technology* **103**(1), 123–130. https://doi.org/10.1016/j.biortech.2011.10.038.

Duman, O., Tunç, S., Bozoğlan, B. K. & Polat, T. G. 2016 Removal of triphenylmethane and reactive azo dyes from aqueous solution by magnetic carbon nanotube-κ-carrageenan-Fe3O4 nanocomposite. *Journal of Alloys and Compounds* **687**, 370–383. https://doi.org/10.1016/j.jallcom.2016.06.160.

Faust, S. D. & Aly, O. M. 2018 *Chemistry of Water Treatment*. CRC Press, USA. https://doi.org/10.1201/9781315139265

Gupta, V., Carrott, P., Ribeiro Carrott, M. & Suhas, D. 2009 Low-cost adsorbents: Growing approach to wastewater treatment- a review. *Critical Reviews in Environmental Science and Technology* **39**, 783–842. https://doi.org/10.1080/10643380801977610.

Hameed, B. H. 2009 Grass waste: A novel sorbent for the removal of basic dye from aqueous solution. *Journal of Hazardous Materials* **166**(1), 233–238. https://doi.org/10.1016/j.jhazmat.2008.11.019.

Hameed, B. H. & El-Khaiary, M. I. 2008a Batch removal of malachite green from aqueous solutions by adsorption on oil palm trunk fibre: Equilibrium isotherms and kinetic studies. *Journal of Hazardous Materials* **154**(1), 237–244. https://doi.org/10.1016/j.jhazmat.2007.10.017.

Hameed, B. H. & El-Khaiary, M. I. 2008b Sorption kinetics and isotherm studies of a cationic dye using agricultural waste: Broad bean peels. *Journal of Hazardous Materials* **154**(1–3), 639–648. https://doi.org/10.1016/j.jhazmat.2007.10.081.

Hariani, P., Faizal, M., Syarofi, R., Marsi, M. & Setiabudidaya, D. 2013 Synthesis and properties of Fe_3O_4 nanoparticles by co-precipitation method to removal procion dye. *International Journal of Environmental Science and Development* **4**, 336–340. https://doi.org/10.7763/IJESD.2013.V4.366.

Hasan, M. M., Shenashen, M. A., Hasan, M. N., Znad, H., Salman, M. S. & Awual, M. R. 2021 Natural biodegradable polymeric bioadsorbents for efficient cationic dye encapsulation from wastewater. *Journal of Molecular Liquids* **323**, 114587. https://doi.org/10.1016/j.molliq.2020.114587.

Hemmateenejad, B., Shamsipur, M., Samari, F. & Rajabi, H. R. 2015 Study of the interaction between human serum albumin and Mn-doped ZnS quantum dots. *Journal of the Iranian Chemical Society* **12**, 1729–1738.

Ho, Y. S. & Mckay, G. 1998 Kinetic models for the sorption of dye from aqueous solution by wood. *Process Safety and Environmental Protection* **76**(2), 183–191. https://doi.org/10.1205/095758298529326.

Hubbe, M., Azizian, S. & Douven, S. 2019 Implications of apparent pseudo-second-order adsorption Kinetics onto cellulosic materials: A review. *BioResources* **14**, 7582–7626. https://doi.org/10.15376/biores.14.3.7582-7626.

Jackson, M., Choo, L. P., Watson, P. H., Halliday, W. C. & Mantsch, H. H. 1995 Beware of connective tissue proteins: Assignment and implications of collagen absorptions in infrared spectra of human tissues. *Biochimica Et Biophysica Acta* **1270**(1), 1–6. https://doi.org/10.1016/0925-4439(94)00056-v.

Ji, Y., Yang, X., Ji, Z., Zhu, L., Ma, N., Chen, D., Jia, X., Tang, J. & Cao, Y. 2020 DFT-calculated IR Spectrum Amide I, II, and III band contributions of N-methylacetamide fine components. *ACS Omega* **5**(15), 8572–8578. Doi:10.1021/acsomega.9b04421.

Kabir, S. M. F., Cueto, R., Balamurugan, S., Romeo, L. D., Kuttruff, J. T., Marx, B. D. & Negulescu, I. I. 2019 Removal of acid dyes from textile wastewaters using fish scales by absorption process. *Clean Technologies* **1**, 311324. https://doi.org/10.3390/cleantechnol1010021.

Khani, O., Rajabi, H. R., Yousefi, M. H., Khosravi, A. A., Jannesari, M. & Shamsipur, M. 2011 Synthesis and characterizations of ultra-small ZnS and Zn(1-x) Fe(x)S quantum dots in aqueous media and spectroscopic study of their interactions with bovine serum albumin. *Spectrochimica Acta. Part A, Molecular and Biomolecular Spectroscopy* **79**(2), 361–369. https://doi.org/10.1016/j.saa.2011.03.025.

Kimura, S., Miyauchi, Y. & Uchida, N. 1991 Scale and bone type I collagens of carp (*Cyprinus carpio*). *Comparative Biochemistry and Physiology Part B: Comparative Biochemistry* **99**, 473–476. https://doi.org/10.1016/0305-0491(91)90073-m.

Kunkun, Z., Gong, X., He, D., Li, B., Ji, D., Li, P. & Peng, Z. 2013 Adsorption of Ponceau 4R from aqueous solutions using alkali boiled Tilapia fish scales. *RSC Advances* **3**, 25221. https://doi.org/10.1039/c3ra43817a.

Laasri, L., Khalid Elamrani, M. & Cherkaoui, O. 2007 Removal of two cationic dyes from a textile effluent by filtration-adsorption on wood sawdust. *Environmental Science and Pollution Research – International* **14**(4), 237–240. https://doi.org/10.1065/espr2006.08.331.

Lagergren, S. K. 1898 About the theory of so-called adsorption of soluble substances. *Sven. Vetenskapsakad. Handingarl* **24**, 1–39.

Langmuir, I. 1918 The adsorption of gases on plane surfaces of glass, mica and platinum. *Journal of the American Chemical Society* **40**(9), 1361–1403. https://doi.org/10.1021/ja02242a004.

Liang, C. Z., Sun, S. P., Li, F. Y., Ong, Y. K. & Chung, T.-S. 2014 Treatment of highly concentrated wastewater containing multiple synthetic dyes by a combined process of coagulation/flocculation and nanofiltration. *Journal of Membrane Science* **469**, 306–315. https://doi.org/10.1016/j.memsci.2014.06.057.

Liu, Y. 2009 Is the free energy change of adsorption correctly calculated? *Journal of Chemical & Engineering Data* **54**(7), 1981–1985. https://doi.org/10.1021/je800661q.

Liu, M., Lü, Z., Chen, Z., Yu, S. & Gao, C. 2011 Comparison of reverse osmosis and nanofiltration membranes in the treatment of biologically treated textile effluent for water reuse. *Desalination* **281**, 372–378. https://doi.org/10.1016/j.desal.2011.08.023.

Mahdi, M., Tuj-Zohra, F. & Ahmed, S. 2021 Dyeing of shoe upper leather with extracted dye from *Acacia nilotica* plant bark – an eco-friendly initiative. *Prog. Color Color. Coat.* **4**, 241–258. https://doi.org/10.30509/pccc.2020.166673.1074.

Maiti, P., Siddiqi, H., Kumari, U., Chatterjee, A. & Meikap, B. C. 2023 Adsorptive remediation of azo dye contaminated wastewater by $ZnCl_2$ modified bio-adsorbent: Batch study and life cycle assessment. *Powder Technology* **415**, 118153. https://doi.org/10.1016/j.powtec.2022.118153.

Marrakchi, F., Ahmed, M. J., Khanday, W. A., Asif, M. & Hameed, B. H. 2017a Mesoporous carbonaceous material from fish scales as low-cost adsorbent for reactive orange 16 adsorption. *Journal of the Taiwan Institute of Chemical Engineers* **71**, 47–54. https://doi.org/10.1016/j.jtice.2016.12.026.

Marrakchi, F., Auta, M., Khanday, W. A. & Hameed, B. H. 2017b High-surface-area and nitrogen-rich mesoporous carbon material from fishery waste for effective adsorption of methylene blue. *Powder Technology* **321**, 428–434. https://doi.org/10.1016/j.powtec.2017.08.023.

Mirmohseni, A., Seyed Dorraji, M. S., Figoli, A. & Tasselli, F. 2012 Chitosan hollow fibers as effective biosorbent toward dye: Preparation and modeling. *Bioresource Technology* **121**, 212–220. https://doi.org/10.1016/j.biortech.2012.06.067.

Mohrazi, A. & Ghasemi-Fasaei, R. 2023 Removal of methylene blue dye from aqueous solution using an efficient chitosan-pectin bio-adsorbent: Kinetics and isotherm studies. *Environmental Monitoring and Assessment* **195**(2), 339. https://doi.org/10.1007/s10661-022-10900-4.

Nassar, M., El Geundi, M. & Al-Wahbi, A. 2012 Equilibrium modeling and thermodynamic parameters for adsorption of cationic dyes onto Yemen natural clay. *Desalination and Water Treatment* **44**, 340–349. https://doi.org/10.1080/19443994.2012.691701.

Nawi, M. A., Sabar, S., Jawad, A. H., Sheilatina & Ngah, W. S. W. 2010 Adsorption of Reactive Red 4 by immobilized chitosan on glass plates: Towards the design of immobilized TiO_2–chitosan synergistic photocatalyst-adsorption bilayer system. *Biochemical Engineering Journal* **49**(3), 317–325. https://doi.org/10.1016/j.bej.2010.01.006.

Neves, C., Scheufele, F., Nardino, A., Vieira, M., Silva, M., Módenes, A. & Borba, C. 2017 Phenomenological modeling of reactive dye adsorption onto fish scales surface in the presence of electrolyte and surfactant mixtures. *Environmental Technology* **39**, 1–17. https://doi.org/10.1080/09593330.2017.1356876.

Ogawa, M., Portier, R. J., Moody, M. W., Bell, J., Schexnayder, M. A. & Losso, J. N. 2004 Biochemical properties of bone and scale collagens isolated from the subtropical fish black drum (*Pogonia cromis*) and sheepshead seabream (*Archosargus probatocephalus*). *Food Chemistry* **88**(4), 495–501. https://doi.org/10.1016/j.foodchem.2004.02.006.

Oladoja, N. A., Aboluwoye, C. O., Oladimeji, Y. B., Ashogbon, A. O. & Otemuyiwa, I. O. 2008 Studies on castor seed shell as a sorbent in basic dye contaminated wastewater remediation. *Desalination* **227**(1), 190–203. https://doi.org/10.1016/j.desal.2007.06.025.

Olivito, F., Algieri, V., Jiritano, A., Tallarida, M. A., Tursi, A., Costanzo, P., Maiuolo, L. & De Nino, A. 2021 Cellulose citrate: A convenient and reusable bio-adsorbent for effective removal of methylene blue dye from artificially contaminated water. *RSC Advances* **11** (54), 34309–34318.

Pavan, F. A., Lima, E. C., Dias, S. L. P. & Mazzocato, A. C. 2008 Methylene blue biosorption from aqueous solutions by yellow passion fruit waste. *Journal of Hazardous Materials* **150**(3), 703–712. https://doi.org/10.1016/j.jhazmat.2007.05.023.

Payne, K. J. & Veis, A. 1988 Fourier transform IR spectroscopy of collagen and gelatine solutions: Deconvolution of the amide I band for conformational studies. *Biopolymers* **27**(11), 1749–1760. https://doi.org/10.1002/bip.360271105.

Ponnusamy, S. K. & Gayathri, R. 2009 Adsorption of Pb^{2+} ions from aqueous solutions onto bael tree leaf powder: Isotherms, kinetics and thermodynamics study. *Journal of Engineering Science and Technology* **4**(4), 381–399.

Ramakrishna, K. R. & Viraraghavan, T. 1997 Dye removal using low-cost adsorbents. *Water Science and Technology* **36**(2), 189–196. https://doi.org/10.1016/S0273-1223(97)00387-9.

Ribeiro, C., Scheufele, F. B., Espinoza-Quiñones, F. R., Módenes, A. N., da Silva, M. G. C., Vieira, M. G. A. & Borba, C. E. 2015 Characterization of *Oreochromis niloticus* fish scales and assessment of their potential on the adsorption of reactive blue 5G dye. *Colloids and Surfaces A: Physicochemical and Engineering Aspects* **482**, 693–701. https://doi.org/10.1016/j.colsurfa.2015.05.057.

Robati, D. 2013 Pseudo-second-order kinetic equations for modelling adsorption systems for removal of lead ions using multi-walled carbon nanotube. *Journal of Nanostructure in Chemistry* **3**(1), 55. https://doi.org/10.1186/2193-8865-3-55.

Saha, P., Chowdhury, S., Gupta, S., Kumar, I. & Kumar, R. 2010 Assessment on the removal of malachite green using tamarind fruit shell as biosorbent. *CLEAN – Soil, Air, Water* **38**(5–6), 437–445. https://doi.org/10.1002/clen.200900234.

Senthilkumaar, S., Varadarajan, P. R., Porkodi, K. & Subbhuraam, C. V. 2005 Adsorption of methylene blue onto jute fiber carbon: Kinetics and equilibrium studies. *Journal of Colloid and Interface Science* **284**(1), 78–82. https://doi.org/10.1016/j.jcis.2004.09.027.

Senturk, H. B., Ozdes, D. & Duran, C. 2010 Biosorption of Rhodamine 6G from aqueous solutions onto almond shell (*Prunus dulcis*) as a low cost biosorbent. *Desalination* **252**(1), 81–87. https://doi.org/10.1016/j.desal.2009.10.021.

Sharma, A. & Bhattacharyya, K. G. 2005 *Azadirachta indica* (Neem) leaf powder as a biosorbent for removal of Cd(II) from aqueous medium. *Journal of Hazardous Materials* **125**(1–3), 102–112. https://doi.org/10.1016/j.jhazmat.2005.05.012.

Shukla, S., Khan, R., Srivastava, M. M. & Zahmatkesh, S. 2023 Valorization of waste watermelon rinds as a bio-adsorbent for efficient removal of methylene blue dye from aqueous solutions. *Applied Biochemistry and Biotechnology*. https://doi.org/10.1007/s12010-023-04448-3.

Tahir, S. S. & Rauf, N. 2006 Removal of a cationic dye from aqueous solutions by adsorption onto bentonite clay. *Chemosphere* **63**(11), 1842–1848. https://doi.org/10.1016/j.chemosphere.2005.10.033.

Tuj-Zohra, F., Ahmed, S., Sultana, R., Nurnabi, M. & Alam, Z. 2022 Removal of Cr(III) from tanning effluent using adsorbent prepared from peanut shell. *Desalination Water Treat.* **266**, 91–100. https://doi.org/10.5004/dwt.2022.28621.

Vieira, E. F. S., Cestari, A. R., Carvalho, W. A., Oliveira, C. D. S. & Chagas, R. A. 2012 The use of freshwater fish scale of the species *Leporinus elongatus* as adsorbent for anionic dyes. *Journal of Thermal Analysis and Calorimetry* **109**(3), 1407–1412. https://doi.org/10.1007/s10973-011-2011-x.

Viscusi, G., Lamberti, E. & Gorrasi, G. 2022 Design of a hybrid bio-adsorbent based on sodium alginate/halloysite/hemp hurd for methylene blue dye removal: Kinetic studies and mathematical modeling. *Colloids and Surfaces A: Physicochemical and Engineering Aspects* **633**, 127925. https://doi.org/10.1016/j.colsurfa.2021.127925.

Von Oepen, B., Kordel, W. & Klein, W. 1991 Sorption of nonpolar and polar compounds to soils processes measurements and experience with the applicability of the modified OECD guideline 106. *Chemosphere* **22**(3–4), 285–304. https://doi.org/10.1016/0045-6535(91)90318-8.

Yunoki, S., Suzuki, T. & Takai, M. 2003 Stabilization of low denaturation temperature collagen from fish by physical cross-linking methods. *Journal of Bioscience and Bioengineering* **96**, 575–577. https://doi.org/10.1016/S1389-1723(04)70152-8.

Zhou, K., Liu, H. & Hao, J. 2012 How to calculate the thermodynamic equilibrium constant using the Langmuir equation. *Adsorption Science & Technology* **30**(7), 647–649.

Zong, E., Fan, R., Hua, H., Yang, J., Jiang, S., Dai, J., Liu, X. & Song, P. 2023 A magnetically recyclable lignin-based bio-adsorbent for efficient removal of Congo red from aqueous solution. *International Journal of Biological Macromolecules* **226**, 443–453.

First received 24 April 2023; accepted in revised form 9 September 2023. Available online 26 September 2023